SUPPORTING INFORMATION

Direct observation and measurement of the average quantum methyl-tunneling frequency in a protein using T_m-edited double electron-electron resonance EPR spectroscopy

Thomas Schmidt,* Francesco Torricella and G. Marius Clore*

Laboratory of Chemical Physics, National Institute of Diabetes and Digestive and Kidney Diseases, National Institutes of Health, Bethesda, MD 20892-0520, U.S.A.

- Experimental Procedures
- 1 Table
- 8 Figures

Experimental Procedures

Expression, purification and labeling of Protein A

AviTag-Protein A, with two surface exposed, engineered cysteine residues (Q39C and K88C) was expressed in *Escherichia coli* and purified as described previously.[1] The AviTag extends from residues 1-29, and Protein A from residues 30-90; residues 1-38 are disordered in solution. Incorporation of protonated methyl groups of Leu ($^{13}C^{\delta1}H_3$ and $^{13}C^{\delta2}H_3$) in a fully deuterated background, {{U[^{2}H]; [Leu-$^{13}CH_3$]}was carried out using standard procedures by growing the bacteria in minimal D_2O (99.9% v/v) medium with ammonium chloride as the sole nitrogen source, U-[^{2}H]-D-glucose as the main carbon source, and α-ketoisovaleric acid (^{13}C5, 98%, 3-D1, 98%) as a precursor for Leu (Cambridge Isotope Laboratories CDLM-4418-PK).{[2-3] (Note there are no valines in AviTag-Protein A). For the uniformly deuterated U[^{2}H] sample, α-ketopisovaleric acid was omitted. Nitroxide (R1p) spin-labeling was carried out with the 3-methanesufonylthiomethyl-4-(pyridine-3-yl)-2,2,5,5-teramethyl-2,5-dihydro-1H-pyrrol-1-yloxyl radical (Toronto Research Chemicals) as described previously.[4-5] R1p spin labeling was characterized by recording an X-band CW EPR spectrum at room temperature and a Q-band echo-detected field swept spectrum at 50 K (Fig. S1). Sample for EPR comprised 50 μM AviTag-Protein A (Q39C-R1p, K88C-R1p) with selective protonation of leucine methyl groups on an otherwise fully deuterated background or complete deuteration, in 0.85 mM KH_2PO_4, 25 mM Na_2HPO_4, pH 7.4, 75 mM NaCl, and d_8-glycerol (30% v/v)/D_2O (70% v/v). For flash-freezing, 15 μL of sample was placed into EPR tubes (1 mm inner diameter, 1.6 mm outer diameter; VitroCom) and plunged directly into liquid nitrogen.

Pulsed Q-band EPR spectroscopy

Pulsed EPR data were collected at Q-band (33.8 GHz) at a temperature of 50 K on a Bruker E-580 spectrometer equipped with a 300 W traveling-wave tube amplifier, a model ER5107D2 resonator, and a cryofree cooling unit, as described previously.[2] T_m-edited DEER experiments were acquired using a conventional four-pulse sequence.[6] The observer and ELDOR pump pulses were separated by ca. 90 MHz with the observer π/2 and π pulses set to 12 and 24 ns, respectively, and the ELDOR π pulse set to 10 ns. The pump frequency was centered at the Q-band nitroxide spectrum located at +40 MHz from the center of the resonator frequency. The τ_1 value of 400 ns for the first echo-period time was incremented eight times in 16 ns steps to average ^{2}H modulation; the position of the ELDOR pump pulse was incremented in steps of Δt = 8 ns. The bandwidth of the overcoupled resonator was 120 MHz. All DEER echo curves were acquired for t_{max} = 4 μs to avoid the persistent "2+1" echo perturbation of the DEER echo curves at a time of about τ_1 from the final observed π pulse, except in those cases where $\tau_2 < 4$ μs, in which case t_{max} was set equal to τ_2. DEER data were recorded with values of the transverse evolution time $T = 2\tau_2$ ranging from 6 to 36 μs for {U-[^{2}H]; Leu-CH_3}-labeled AviTag-Protein A, and 4 to 32 μs for U-[^{2}H]-labeled AviTag-Protein A.

Prediction of R1p positions using the CalcPr function in Xplor-NIH. A description of the CalcPr function has been previously provided in refs. 7 and 8. Briefly, the R1 (assumed to be the same for R1p) conformations are represented by 20 relative positions and associated weights obtaining by directly fitting many X-band DEER echo curves previously recorded by H.S. McHaourab and J. Meiler for many T4 lysozyme nitroxide labeled samples.[9] The effective weight of each conformer position is modulated (multiplied) by a term which accounts for occlusion due to steric clash with the protein backbone. Each pair of R1 conformers gives a contribution to the pair distance distribution, $P(r_{ee})$, of a fixed width, corresponding to distributions in the positions of both conformers.

Table S1. Values of the optimized global parameters obtained from a global 2-Gaussian fit to the T_m-edited DEER data for {U-[^{2}H]; [Leu-[^{13}CH$_3$]} and U-[^{2}H]-labeled Protein A (Q39C-R1p/K88C-R1p).[a]

	Isotope labeling	
	{U-[^{2}H]; [Leu-[^{13}CH$_3$]}	U-[^{2}H]
Deer time traces	31	30
Total number of data points	18275	16557
Normalized χ^2	1.3	1.3
Unpaired electron – unpaired electron dipolar interaction (r_{ee})		
Gaussian 1		
mean distance (Å)	32.2 ± 0.1	32.3 ± 0.1
peak width (Å)[d]	0.9 ± 0.1	0.9 ± 0.1
Gaussian 2		
mean distance (Å)	38.1 ± 0.1	38.3 ± 0.1
peak width (Å)[d]	2.1 ± 0.1	2.1 ± 0.1

[a]The local optimized parameters are the modulation depth and the decay rate constant for the exponential background function which are specific to each individual DEER echo curve.
[b]The peak width is defined as the full-width at half the maximum height of the distance peak.

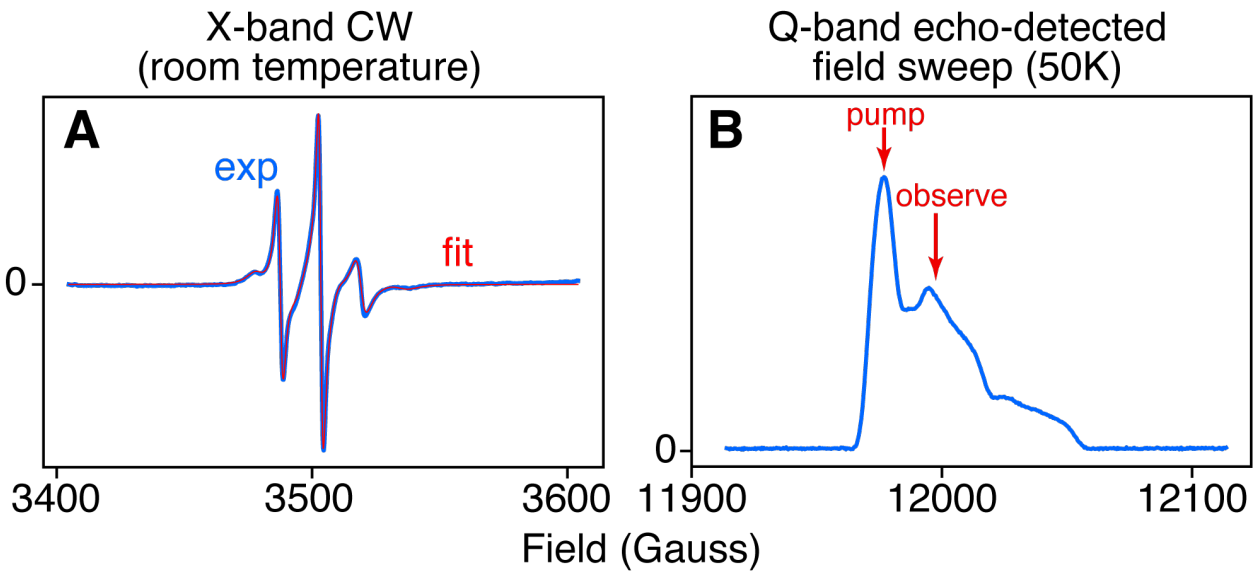

Figure S1. Characterization of R1p spin-labeling of deuterated AviTag-Protein A (Q39C/R88C) by X-band CW and Q-band echo-detected field sweep EPR. (A) Room temperature X-band (9.3 GHz) CW spectra of fully deuterated aviTag-protein A, R1p spin-labeled at Q39C and K88C. Data were recorded on a Bruker Elexsys E580 spectrometer equipped with a SHQE resonator (kindly made available to us by Dr. Veronika Szalai, National Institutes of Standards and Technology, NIST) using a spectral scan width of 200 G. The experimental data are shown in blue and a two-component fit (red) was carried out using the program EasySpin (https://easyspin.org)[10]: the population and correlation time are 1.1 ns and 49.4%, respectively, for the narrow component, and 7.6 ns and 50.6%, respectively, for the broad component. The narrow and broad components arise from the R1p label attached to Q39C and K88C, respectively; note the latter is in a highly mobile disordered C-terminal tail and hence the attached R1p label samples a wide region of conformational space. (B) Q-band (33.8 MHz) echo-detected field sweep EPR spectrum at 50 K for fully deuterated aviTag-protein A (Q39C-R1p/K88C-R1p). The red arrows indicate the positions of the pump and observe pulses used in the DEER experiments. A Hahn echo with $\pi/2$ and π pulses of 12 and 24 ns, respectively, a half echo period of 400 ns, and an integration window of 32 ns was used to collect the Q band data. The Q-band data were acquired on a Bruker E-580 spectrometer equipped with a 150 W traveling-wave tube amplifier, a model ER5107D2 resonator, and a cryofree cooling unit operating at 50 K. Introducing leucine methyl protonation on a fully deuterated background has no detectable impact on the X-band CW or Q band echo-detected field sweep spectra.

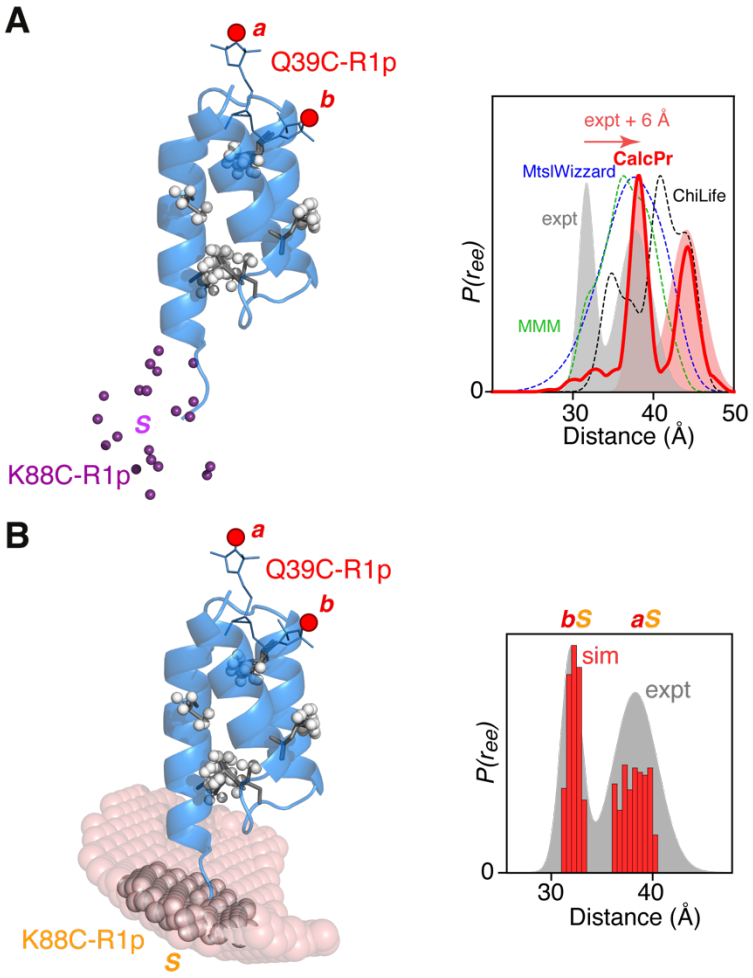

Figure S2. Comparison of the experimental DEER-derived $P(r_{ee})$ distribution for {U-[^{2}H]; Leu-[$^{13}CH_3$]}-labeled protein A (Q39C-R1p/K88C-R1p) with predicted $P(r_{ee})$ distributions from the crystal structure. (A) (Left) Positions of the Q39C-R1p (large red spheres) and K88C-R1p (purple spheres) predicted using the rotamer library employed in the CalcPr module[7-8] of the program Xplor-NIH[11-12] displayed on a ribbon diagram (light blue) of protein A with the methyl groups of the leucines depicted as white spheres. (Right) Comparison of the experimental DEER-derived $P(r_{ee})$ distribution (shaded grey) with the calculated distributions based on the X-ray coordinates (PDB code 4NPE)[13] using the CalcPr (rotamer library based) function[7] in Xplor-NIH[11-12] (thick red line), as well as various other programs (MMM,[14-15] green dashed lines; ChiLife,[16] black dashed lines; and MtslWizzard,[17] blue dashed lines). Only CalcPr predicts the clear bimodal distribution observed experimentally. However, the peaks in the CalcPr distribution (as well as the other calculated distributions) are about 6 Å longer than the experimental P(r_{ee}) distribution. This is due to the fact that the predicted position of K88C-R1p is based on fixed crystal coordinates for the last 2 residues which are in fact highly mobile in solution. When the CalcPr predicted distribution is shifted by 6 Å (shaded red), the match to the two experimental DEER distance peaks is extremely good. (B) Spatial distribution of the oxygen atom bearing the unpaired electron of the K88C-R1p label (left, pink spheres) that is fully consistent with the experimental $P(r_{ee})$ distribution (right, with the summed distances between the R1p spin centers shown in red with a bin size of 0.5 Å). (The darked-shaded pink spheres represent the space that can potentially be sampled with the C-terminal residues fixed at their positions in the crystal structure with a maximum R1p linker distance of 7 Å from the Cα of K88C to the unpaired electron-bearing oxygen of R1p).

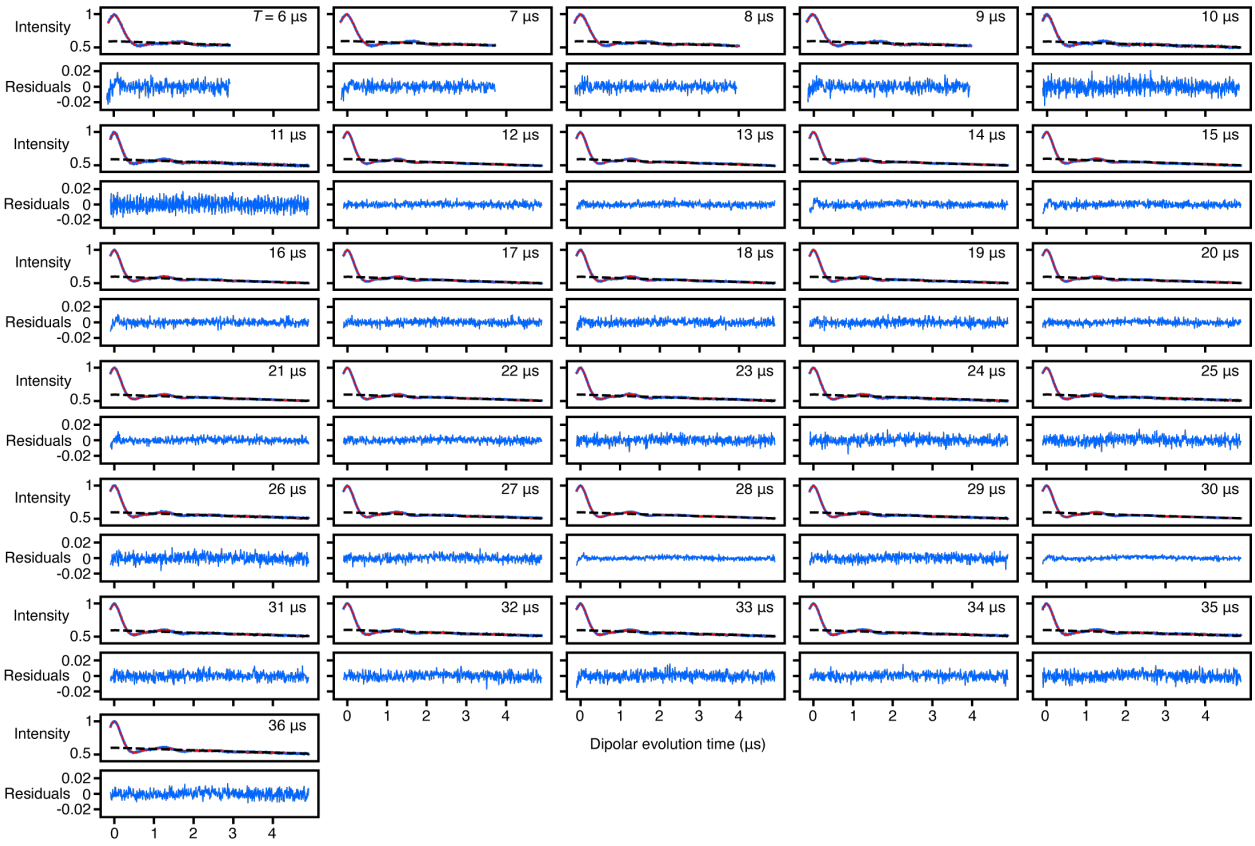

Figure S3. Analysis of Q-band T_m-edited DEER data acquired for {U-[^{2}H]; Leu-[$^{13}CH_3$]}-labeled protein A (Q39C-R1p/K88C-R1p) using model-free Tikhonov regularization. In each panel, the top half displays the experimental (blue) and bestfit (red) DEER echo curves, with the background displayed as a dashed line; the bottom half shows the corresponding residuals between experimental and calculated curves. The data at each evolution time $T = 2\tau_2$ delay (T = 6 to 36 µs) were fitted individually using validated Tikhonov regulation in the program DeerLab with bootstrap analysis for uncertainty quantification via the bootan function in the DeerLab library with the number of bootstrap samples n = 1000.[18]

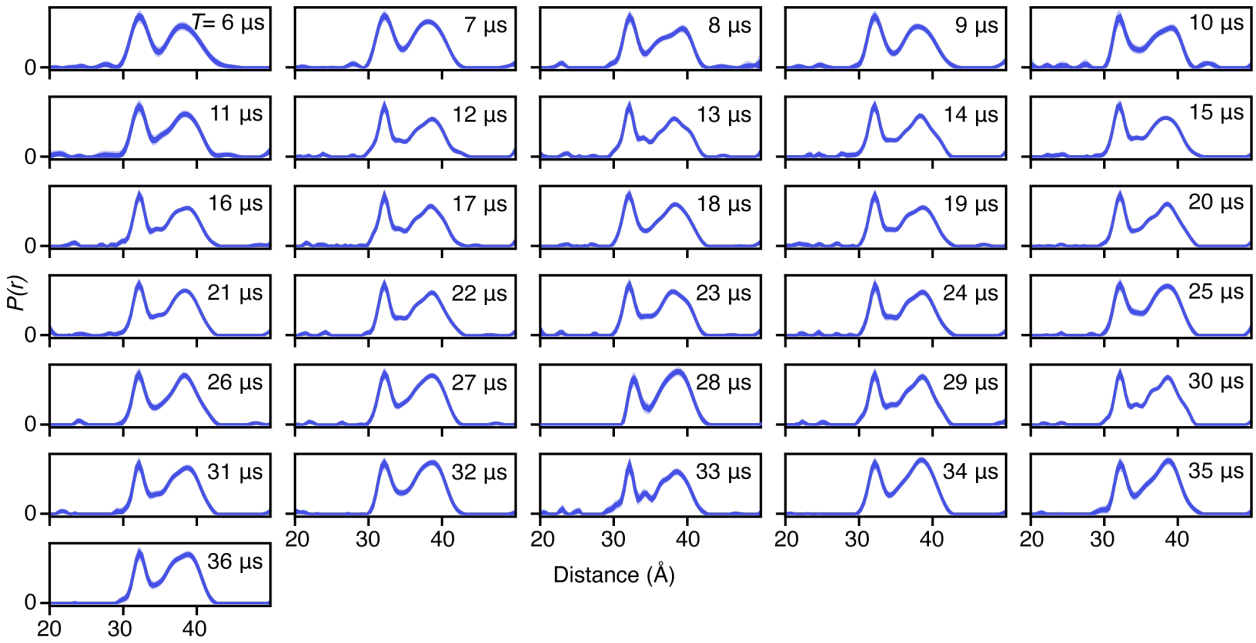

Figure S4. DEER-derived $P(r_{ee})$ distributions for {U-[^{2}H]; Leu-[$^{13}CH_3$]}-labeled protein A (Q39C-R1p/K88C-R1p) for evolution times T ranging from 6 to 36 µs obtained by validated Tikhonov regularization. The bestfits to the individual experimental T_m-edited DEER echo curves are shown in Fig. S3. The shaded regions delineate the 95% (*light blue*) and 50% (*dark blue*) confidence intervals.

Figure S5. Global analysis of Q-band T_m-edited DEER data for T = 6 to 36 µs obtained for {U-[^{2}H]; Leu-[$^{13}CH_3$]}-labeled protein A (Q39C-R1p/K88C-R1p), using a 2-Gaussian fit. In each panel, the top half displays the experimental (blue) and bestfit (red) DEER echo curves; the bottom half shows the corresponding residuals between experimental and calculated curves. The data at all evolution times T = $2\tau_2$ delay were fitted simultaneously with the peak positions and corresponding peak widths in the $P(r_{ee})$ distribution treated as global parameters using an in-house Python script[7-8] based on the program DD/GLADDvu.[19-20]

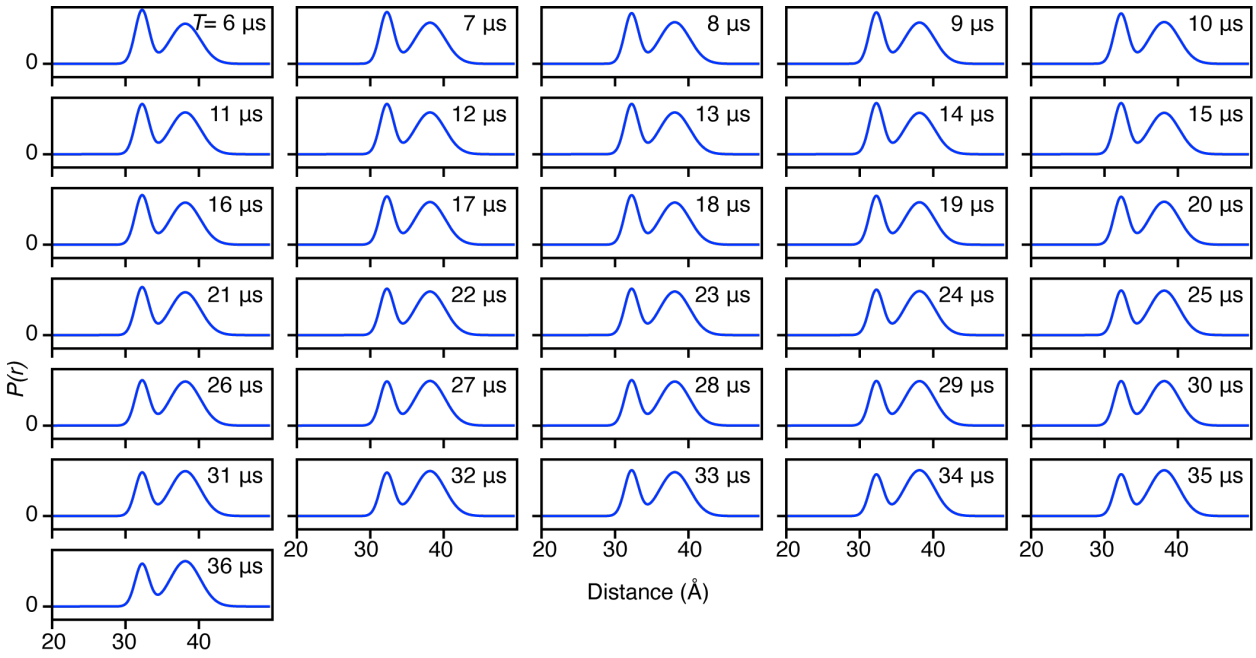

Figure S6. T_m-edited DEER-derived $P(r_{ee})$ distributions obtained for {U-[^{2}H]; Leu-[$^{13}CH_3$]}-labeled protein A (Q39C-R1p/K88C-R1p) for evolution times T ranging from 6 to 36 µs using a 2-Gaussian global fit in which the peak positions and corresponding widths of the $P(r_{ee})$ distribution are treated as global parameters (see main text for details). The bestfits to the experimental DEER echo curves are shown in Fig. S5.

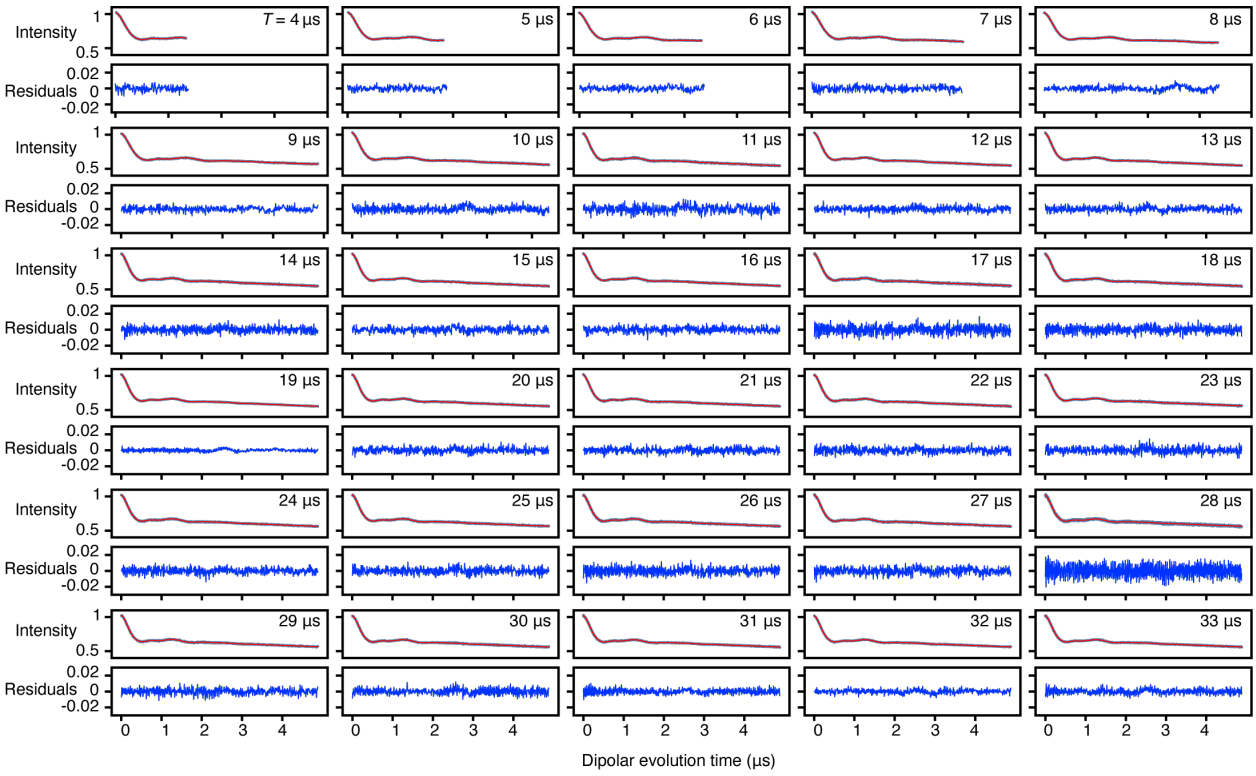

Figure S7. Global analysis of Q-band T_m-edited DEER data obtained for {U-[^{2}H]; Leu-[$^{13}CH_3$]}-labeled protein A (Q39C-R1p/K88C-R1p) for evolution times T ranging from 4 to 33 µs. In each panel, the top half displays the experimental (blue) and bestfit (red) DEER echo curves; the bottom half shows the corresponding residuals between experimental and calculated curves. The data at all evolution times $T = 2\tau_2$ were fit simultaneously with the peaks positions and widths of the $P(r_{ee})$ distribution, the apparent T_m^{app}, and the peak position and width of the $P(r_{eH})$ distribution were treated as global parameters using an in-house Python script[7-8] based on the program DD/GLADDvu.[19-20] (see main text for details, as well as Eq. 9 and Table 1 in the main text).

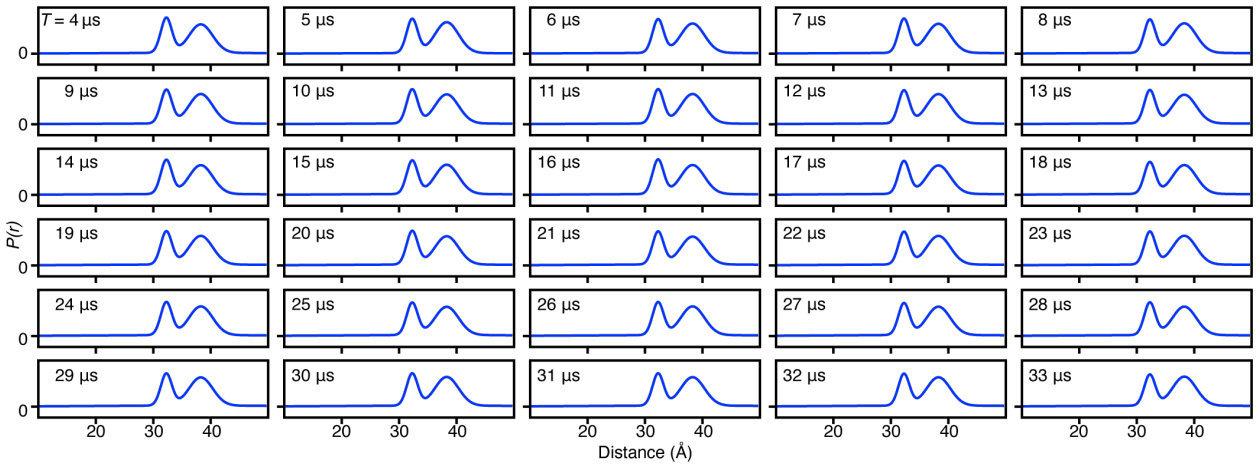

Figure S8. T_m-edited DEER-derived *P(r_{ee})* distributions obtained for {U-[^{2}H]; Leu-[$^{13}CH_3$]}-labeled protein A (Q39C-R1p/K88C-R1p) for evolution times *T* ranging from 4 to 33 µs using a 2-Gaussian global fit in which the peaks positions and widths of the $P(r_{ee})$ distribution, the apparent T_m^{app}, and the peak position and width of the $P(r_{eH})$ distribution were treated as global parameters (see main text for details as well as Eq. 9 and Table 1 of the main text). The bestfits to the experimental DEER echo curves are shown in Fig. S7.

Supplementary References

1 J. L. Baber, J. M. Louis and G. M. Clore, *Angew. Chem. Int. Ed. Engl.* 2015, **54**, 5336-5339.
2 T. Schmidt and G. M. Clore, *Chem. Commun. (Camb.)* 2020, **56**, 10890-10893.
3 V. Tugarinov and L. E. Kay, *J. Biomol. NMR* 2004, **28**, 165-172.
4 N. L. Fawzi, M. R. Fleissner, N. J. Anthis, T. Kalai, K. Hideg, W. L. Hubbell and G. M. Clore, *J. Biomol. NMR* 2011, **51**, 105-114.
5 T. Schmidt and V. Stadnytskyi, *Appl. Magn. Reson.* 2025, **56**, 91-102.
6 M. Pannier, S. Veit, A. Godt, G. Jeschke and H. W. Spiess, *J. Magn. Reson.* 2000, **142**, 331-340.
7 T. Schmidt, J. Jeon, W. M. Yau, C. D. Schwieters, R. Tycko and G. M. Clore, *Proc. Natl. Acad. Sci. U. S. A.* 2022, **119**, e2122308119.
8 T. Schmidt, D. Wang, J. Jeon, C. D. Schwieters and G. M. Clore, *J. Am. Chem. Soc.* 2022, **144**, 12043-12051.
9 D. Del Alamo, M. H. Tessmer, R. A. Stein, J. B. Feix, H. S. McHaourab and J. Meiler, *Biophys. J.* 2020, **118**, 366-375.
10 S. Stoll and A. Schweiger, *J. Magn. Reson.* 2006, **178**, 42-55.
11 C. D. Schwieters, J. J. Kuszewski, N. Tjandra and G. M. Clore, *J. Magn. Reson.* 2003, **160**, 65-73.
12 C. D. Schwieters, G. A. Bermejo and G. M. Clore, *Protein Sci.* 2018, **27**, 26-40.
13 L. N. Deis, C. W. t. Pemble, Y. Qi, A. Hagarman, D. C. Richardson, J. S. Richardson and T. G. Oas, *Structure* 2014, **22**, 1467-1477.
14 G. Jeschke, *Protein Sci.* 2018, **27**, 76-85.
15 G. Jeschke, *Protein Sci.* 2021, **30**, 125-135.
16 M. H. Tessmer and S. Stoll, *PLoS Comput. Biol.* 2023, **19**, e1010834.
17 G. Hagelueken, R. Ward, J. H. Naismith and O. Schiemann, *Appl. Magn. Reson.* 2012, **42**, 377-391.
18 L. Fabregas Ibanez, G. Jeschke and S. Stoll, *Magn. Reson. (Gott.)* 2020, **1**, 209-224.
19 S. Brandon, A. H. Beth and E. J. Hustedt, *J. Magn. Reson.* 2012, **218**, 93-104.
20 E. J. Hustedt, R. A. Stein and H. S. McHaourab, *J. Gen. Physiol.* 2021, **153**, e201715994.